

Incorporation of alkali metals on Pt(111)

J. Lehmann, P. Roos, and E. Bertel

Max-Planck-Institut für Plasmaphysik, Abteilung Oberflächenphysik, EURATOM Association, D-85740 Garching, Germany

(Received 15 April 1996, revised manuscript received 20 May 1996)

The alkali-metal-doped platinum (111) surface is one of the most popular model systems for studies on catalytic promotion. Our results indicate that in the low-coverage range the alkali metals Na and K are incorporated into the surface. This is in contrast to the widely accepted adsorption geometry and calls for the reexamination of the current picture of alkali-metal-coadsorbate interactions on Pt(111). The driving mechanism for the incorporation is apparently different from that known on other metal surfaces and may be related to the large surface stress of Pt(111). [S0163-1829(96)51728-5]

The present understanding of alkali-metal-induced promotion mechanisms in heterogeneous catalysis is largely based on the study of model systems. Among such systems K/Pt(111) plays an exceptional role. It is probably the most frequently used model surface for the investigation of coadsorption effects^{1,2} and the alkali-induced bond weakening of CO. An exact knowledge of the adsorption geometry is essential for understanding alkali-metal-induced promotion³ in particular and the properties of alkali-doped metal surfaces in general.⁴ The present study demonstrates that for Pt(111) the generally assumed alkali-metal adsorption geometry is inconsistent with experimental data. Consequently, current models for coadsorbate interactions on alkali-doped Pt(111) have to be critically reexamined.

Existing studies of the K/Pt(111) system indicate a behavior thought to be characteristic for alkali-metal adsorption: At low coverage adsorption with a large dipole moment and strong repulsive interaction, at larger coverages eventual metallization and formation of ordered adsorbate overlayers. In contrast, the present measurements including temperature programmed desorption (TPD), work function ($\Delta\Phi$) measurements, Auger electron spectroscopy (AES), as well as Xe TPD and photoemission of adsorbed Xe (PAX), indicate incorporation of a substantial amount of the alkali atoms during the initial stages of exposure. At higher coverages, the system reverts to normal behavior. The discrepancy with earlier measurements stems from an extremely sharp desorption feature at high temperature which is partly due to ionic desorption not detected in previous experiments. As a consequence, the coverage at the early adsorption stages was consistently underestimated.

The experiments were carried out in a uHV system with a base pressure of 10^{-10} mbar. The Pt crystal was mounted on a cryogenic manipulator. Temperatures were measured by a Ni-CrNi thermocouple and the temperature reading in the low-temperature range was calibrated by Xe desorption measurements using the data of Kern *et al.*⁵ The sample cleaning was already described in Ref. 6. Alkali metals were dosed by means of an SAES getter source, which was mounted inside a heated glass collimator tube. During exposure, the pressure in the vacuum chamber remained below 4×10^{-10} mbar. The work function was determined from the total width of the photoemission spectrum ($h\nu = 16.85$ eV, sample bias: -5 eV). A four-grid low-energy electron diffraction (LEED) op-

tics was used for measuring the Auger spectra. Temperature programmed desorption (TPD) spectra were recorded by means of a retractable quadrupole mass spectrometer (QMS) with the entrance aperture ($\varnothing \approx 3$ mm) positioned 5 mm in front of the sample surface.

Figure 1 shows a TPD spectrum (heating rate 3.4 K s^{-1}) obtained from about two monolayers of potassium on Pt(111). The structure at 350 K on the high-energy side of the multilayer desorption peak is attributed to desorption from the compressed first monolayer with a coverage of $\Theta = 0.44$.⁷ Beyond 400 K the desorption rate is low, but on an enlarged scale a peak at 600 K is observed in agreement with other groups.⁸⁻¹⁰ At 1000 K the desorption rate rises again to an extremely sharp, intense maximum at 1100 K with a full width at half maximum (FWHM) of only 13 K, while the hitherto published TPD spectra show only a small increase in the desorption rate at this temperature. The sharp peak at 1100 K contains a large fraction of desorbing ions, which is responsible for a major part of the signal. Previous TPD spectra⁸⁻¹⁰ were recorded by use of detectors which suppressed positive ions, namely either by a UTI QMS,^{8,10} where the ion source is held at a positive potential, or by a surface ionization detector⁹ which rejected the desorbing ions. In contrast, a HIDDEN QMS with an ion source at negative potential was used in the present experiment. In addition, heating rates in previous TPD experiments were higher by a factor of 5–10. The resulting unfavorable desorption rate-pumping speed ratio leads to considerable broadening

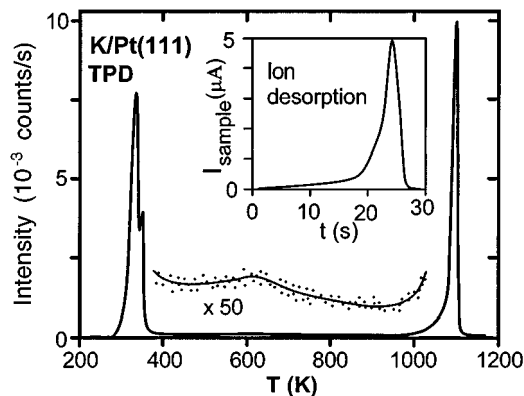


FIG. 1. Temperature programmed desorption spectrum of about 2 ML of K from Pt(111) (heating rate 3.4 K s^{-1}). The signal at 1100 K stems predominantly from ionic desorption. Inset: Sample current measured during desorption. A measurable sample current appears only around 1100 K.

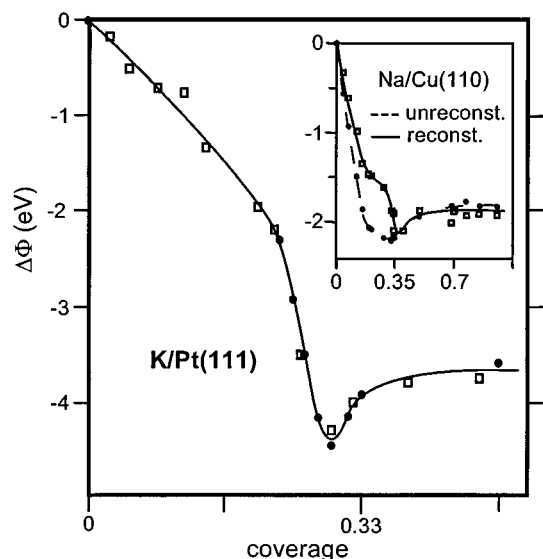


FIG. 2. K-induced work function change on Pt(111). Solid circles: Coverages prepared via thermal desorption of excess K. Open squares: Coverages prepared via direct dosing at $T < 140$ K. Inset: Work function change measured for Na on Cu(110) after annealing to 370 K, which induces a missing row reconstruction (solid line) and after adsorption at 100 K, where the reconstruction is suppressed (Ref. 14) (dashed line).

and renders detection of very sharp TPD features difficult.

To derive the coverage scale from the TPD spectra we calibrated the relative sensitivity of the QMS towards ions and neutrals. First, the absolute number of desorbing ions was determined from integrating the sample current measured during a desorption cycle (Fig. 1, inset) and normalizing to unit sample area.¹¹ For $\Theta > 0.3$ the ion desorption peak saturated. The corresponding charge was equivalent to 1.2×10^{14} desorbed particles per cm^2 . A comparison to the MQS signal obtained with the ionizer filament switched off yielded the MQS sensitivity towards positive ions. The absolute number of desorbing neutrals was calculated from the known coverage in a $(\sqrt{3} \times \sqrt{3})R30^\circ$ adsorbate layer (i.e., $5.0 \times 10^{14} \text{ cm}^{-2}$) minus the number of desorbing ions. This neutral desorption yield was then compared to the difference in the integrated MQS signals obtained with and without filament emission, respectively, in TPD spectra starting from the saturated $(\sqrt{3} \times \sqrt{3})R30^\circ$ structure.¹² The latter was reproducibly prepared by annealing a potassium covered sample to 400 K. An MQS ion-to-neutral sensitivity ratio of 3.4 was obtained in this way (this ratio depends not only on the ionization probability of K in the ion source, but also on the imaging conditions for the K^+ ions in the ion optical system of the MQS). The extremely narrow peak at 1100 K seems to originate from an autocatalytic desorption mechanism, because the desorption rate kept increasing despite falling temperature as the heating was switched off after ramping to 1075 K. This is consistent with the peculiar upward shift of the high temperature edge of the neutral desorption signal with increasing coverage^{8,10} observed by other groups.

Figure 2 shows the K-induced work function change. For clean Pt(111) we obtained a work function of 5.97 eV. Different coverages were prepared by either directly dosing the sample with the required amount at low temperature or by annealing the sample with a multilayer precoverage at a cer-

tain temperature to remove the excess K. Both preparation methods yielded the same work function changes. The present result differs significantly from published K/Pt(111) work function curves,^{10,13} which show a continuous work function drop towards the minimum with a gradually decreasing slope due to depolarization effects. Instead, we observed a pronounced discontinuity of the slope at $\Theta = 0.22$. The shape is reminiscent of adsorption on reconstructing surfaces as shown in the inset of Fig. 2. For Na on Cu(110), regular adsorption results in the usual work function curve. In contrast, substitutional adsorption after annealing to 360 K (Ref. 14) yields an initially smaller slope due to the reduced dipole moment of the substitutionally adsorbed alkali atoms and a subsequent fast drop. By analogy, the work function curve for K on Pt(111), too, indicates incorporation into the surface layer or even absorption into subsurface sites. The coverage at the breaking point of the work function curve corresponds exactly to that obtained by removing excess potassium via flash desorption up to 1000 K. In view of these results we associate the narrow autocatalytic desorption peak at 1100 K with a deconstruction initiated by further K removal. Similar sharp desorption features occur during the deconstruction of H-induced reconstructions.¹⁵

For $\Theta > 0.25$ we observe the usual sequence of (2×2) , $(\sqrt{3} \times \sqrt{3})R30^\circ$, and compression LEED patterns up to the $(3/2 \times 3/2)$ pattern characteristic of the full compressed monolayer.⁷ The latter coincides with the onset of the multilayer peak in TPD just below 350 K. In the range $0.25 < \Theta < 0.44$ the coverage scale derived from LEED and TPD agree perfectly. In view of the LEED pattern sequence and the correspondence of LEED and TPD coverage scales a surface alloy formation seems unlikely. Beyond $\Theta = 0.25$ the majority of the alkali atoms obviously occupies regular adsorption sites. As exposure at low temperature and removal of excess K by thermal desorption yields the same work function values for corresponding coverages, the phase transition at $\Theta = 0.22$ is apparently reversible.

Next we measured the K(252 eV)/Pt(237 eV) AES peak ratio as a function of coverage for the two different preparation conditions (Fig. 3). Usually, the K AES signal is normalized to the Pt(64 eV) peak. We choose the Pt(237 eV) peak because the background in the low-energy range of the AES spectrum changed considerably during K adsorption. A small K AES feature overlapping the Pt(237 eV) peak influences the AES uptake curve only at very large K coverages. The AES measurements reflect the same discontinuity as the work function curve at $\Theta = 0.22$. Up to this point the AES signal increases very slowly, but for $0.22 < \Theta < 0.30$ a fast increase is observed. If the coverages are prepared by direct dosing at temperatures below 140 K, the measured AES intensities show a comparatively large scatter in this coverage region. Preparation by annealing, in contrast, reduces the scatter, and the measured AES intensities lie on a sigmoidal curve. This supports the conclusions drawn already from the work function change, namely initial incorporation of the K atoms and subsequent reversion to regular adsorption as a critical coverage of $\Theta = 0.22$ is exceeded. It is important to note that a plot of the AES peak ratio versus time of exposure results in a curve, which is linear throughout the first monolayer range, but bends upward as the second monolayer begins to form. This is the curve shape usually reported in

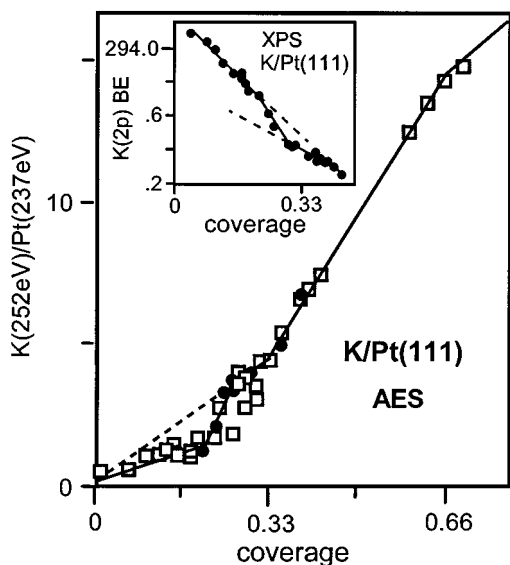


FIG. 3. Auger peak intensity ratio $K(252\text{ eV})/Pt(237\text{ eV})$ as a function of K coverage on Pt(111). Solid circles: Coverages prepared via thermal desorption of excess K. Open squares: Coverages prepared via direct dosing at $T < 140\text{ K}$. The solid line serves as a guide to the eye, the broken line indicates the shape of the AES uptake curve as given in the literature. Inset: K $2p$ binding energy shift as a function of coverage (Refs. 9 and 10). [Pirug and Bonzel (Ref. 16).]

the literature.^{9,10} According to our coverage calibration, however, the sticking coefficient drops to $\frac{1}{3}$ of its initial value for coverages beyond $\Theta = 0.22$.

Our scenario for the first adsorption stages involving an incorporation of the alkali metal into the Pt(111) surface is in marked contrast to the prevailing picture. The discrepancy arises because in previous studies the sharp high-temperature desorption peak was not properly resolved and the ion yield neglected. Consequently, the initial coverage was severely underestimated, while the $\sqrt{3} \times \sqrt{3} R19.1^\circ$ LEED pattern provided a fixed calibration point close to monolayer saturation. The resulting nonlinear distortion of the coverage scale masked the discontinuity at $\Theta = 0.22$.

At coverages below $\Theta = 0.25$ Schweizer¹⁶ as well as Pirug and Bonzel⁷ reported the observation of a remarkably unstable and radiation sensitive $(\sqrt{7} \times \sqrt{7})R19.1^\circ$ LEED pattern in a very narrow coverage range followed by “ring” patterns with elongated split spots. The latter pattern gradually changed into the (2×2) structure as the coverage increased. While the LEED patterns are qualitatively consistent with our observations, we assign the LEED sequence to a different coverage range. A coverage of 0.14 ML obtained from the conventional AES uptake curve given as the broken line in Fig. 3 transforms to an actual coverage of $\Theta = 0.22$ in our calibration. This is just the critical coverage, where our data indicate the onset of a transition towards regular adsorption. The sequence of LEED patterns between the $(\sqrt{7} \times \sqrt{7})R19.1^\circ$ and the (2×2) structure corresponds therefore to the coverage range where we observe a temperature dependent behavior of the AES signal indicating structural rearrangement. A possible interpretation of the LEED sequence would then be as follows: At $\Theta = 0.22$ the alkali atoms start to return into regular adsorption sites on the surface forming $(\sqrt{7} \times \sqrt{7})R19.1^\circ$ islands under appropriate

conditions. As there is still a reservoir of subsurface alkali atoms, this structure is extremely radiation sensitive and can easily be destroyed, if the temperature is increased.⁷ The “ring” pattern could then on the one hand be due to a regularly adsorbed, azimuthally disordered alkali atom overlayer which is gradually compressed into the (2×2) structure. On the other hand, it cannot be excluded that the sequence of LEED patterns is produced by a mixed alkali-metal–Pt overlayer. For instance, part of the alkali metals could occupy substitutional sites in a $(\sqrt{7} \times \sqrt{7})R19.1^\circ$ structure, and an incommensurate “floating” alkali-metal–Pt overlayer could develop at higher coverages giving rise to the ring patterns. An alkali-metal-induced decoupling of the top layer from the substrate was actually observed for Na on Au(111).¹⁷ It is important to note that in both models sketched here the 0.14-ML coverage associated with the $(\sqrt{7} \times \sqrt{7})R19.1^\circ$ structure does not correspond to the actual alkali-metal coverage because of the coexistence with other phases, for instance subsurface alkali-metal atoms. This is analogous to Na/Au(111),¹⁸ where, for example, a (2×2) pattern was observed up to coverages of 0.45 ML. In the latter case, too, the structure was attributed to a coexistence of two different adsorption sites, namely substitutionally and regularly adsorbed Na. The presence of at least two inequivalent adsorption sites can also be inferred from the fact that the phase transition occurs at a coverage as large as 0.22. Such an amount of atoms can hardly be accommodated within purely substitutional or interstitial sites as long as only surface alloy formation takes place.

Further support for the present conclusion stems from the literature. The inset in Fig. 3 shows the $K(2p)$ XPS binding energy shift measured by Pirug and Bonzel.⁷ The data are clearly consistent with a phase transition occurring at $0.22 < \Theta < 0.30$. Even more striking is that a dramatic decrease of the sticking coefficient for CO in exactly this coverage range has been reported.^{13,19} Either a change in the associated lifetime of a supposed CO precursor¹³ or an increase of the K radius and a more efficient site-blocking¹⁹ was invoked. Similar effects, however, were not observed on other alkali-metal adsorption systems. In the present scenario the sudden drop of the CO sticking coefficient is quite naturally rationalized by the transition from incorporated to regularly adsorbed potassium.

In search of independent evidence we have also carried out photoemission and TPD measurements of Xe adsorbed on K/Pt(111) (Fig. 4). At K precoverages below $\Theta = 0.22$ the Xe photoemission spectra are characterized by a splitting of the Xe $5p_{1/2}$ peak²⁰ as shown in the lower spectrum of Fig. 4. The work function of the corresponding K/Pt(111) surface was 4 eV ($\Delta\Phi_K = -1.95\text{ eV}$, $\Theta_K = 0.20$). Beyond the breaking point in the work function curve an additional component appears in the Xe $5p_{1/2}$ spectrum, as shown in the upper spectrum of Fig. 4 ($\Delta\Phi_K = -2.31\text{ eV}$, $\Theta_K = 0.23$). This dramatic change of the peak shape within a narrow coverage range provides independent evidence for a phase transition taking place as the critical coverage is exceeded. The conclusions are further supported by the Xe TPD data. Up to $\Theta_K = 0.22$ the Xe adsorption energy remains by and large the same as on the clean surface (see inset of Fig. 4). Beyond $\Theta_K = 0.27$ no Xe at all could be adsorbed at temperatures

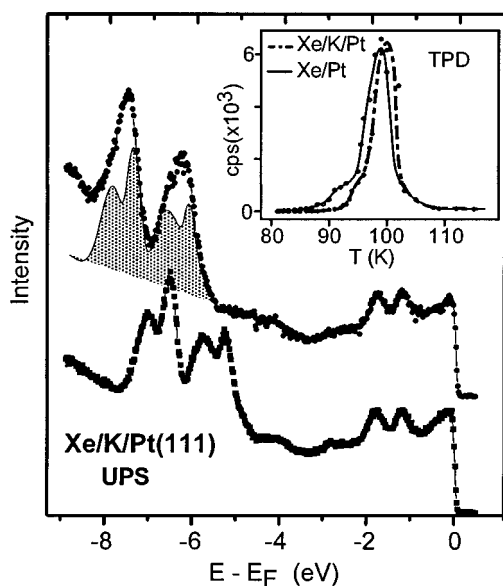


FIG. 4. Photoemission measurements on adsorbed Xe (PAX). Lower spectrum: K/Pt(111) surface prepared by annealing to 1070 K ($\Theta_K=0.20$), Xe saturation exposure. Upper spectrum: K/Pt(111) surface prepared by annealing to 1000 K ($\Theta_K=0.23$), Xe saturation exposure. Shaded curve: Xe 5p emission taken from the lower spectrum and shifted by 0.83 eV. Inset: Xe TPD spectra from clean Pt(111) (solid curve) and from K/Pt ($\Theta_K=0.22$) (dash-dotted line).

down to 60 K and pressures up to 7×10^{-7} mbar, which is the behavior generally observed on alkali covered surfaces.²¹

We obtained very similar data concerning TPD work function measurements, and PAX for Na/Pt(111). All these results strongly suggest that the light alkali metals are incorporated at coverages below $\Theta=0.22$. At higher coverages they revert to regular adsorption as indicated by the compression structures observed in LEED. As the incorporation is also observed at 100 K, the activation energy has to be very low.

A change of adsorption site as a function of coverage has been observed for alkali metals on Ru(0001) as well.²² In

this case, however, the site change was associated with the transition between different ordered superstructures at coverages above $\Theta=0.25$ and involved only a transfer from fcc or on-top to hcp sites. Such a site change could hardly explain the present work function and AES data, which suggest a true incorporation. In view of the small activation energy an interstitial incorporation seems more likely than a substitutional one in contrast to other close-packed metal surfaces,²³ for instance Na/Al(111) (Ref. 24) or Na/Au(111),²⁵ where substitutional adsorption has been found. However, the data suggest that inequivalent adsorption sites are simultaneously populated. We speculate that in the present case the driving force for the incorporation is associated with the large surface stress of the Pt(111) surface.²⁶ At low coverages incorporation of the alkali atoms may lead to an efficient stress release. The present results should be compared to those of Ertl and co-workers¹⁸ for Na adsorption on Au(111). The TPD spectrum from this system looks strikingly similar to that shown here in Fig. 1. The sharp high-temperature desorption feature is attributed to the decomposition of a mixed NaAu₂ phase. On Au(111) the peak does not saturate, because at higher coverages a NaAu₂ bulk alloy is formed. This is not possible in the alkali metal/Pt(111) system, but the similar TPD spectrum strongly supports the assumption of the formation of a mixed surface phase. Due to the large surface stress on Pt(111) the mixed phase may form spontaneously, while on Au(111) the formation of this phase requires a finite coverage and thermal activation, because already on the clean surface the stress is released via the $22 \times \sqrt{3}$ reconstruction. On K(Na)/Pt(111) the details of the incorporation mechanism have yet to be clarified, but the peculiar properties of the system indicate that the mechanism is different from what has been observed in other alkali-metal adsorption systems so far.

We gratefully acknowledge continuous support by V. Dose, useful discussions with G. Rangelov, and technical assistance by E. Berger. This work was supported in part by the Deutsche Forschungsgemeinschaft.

¹J. E. Müller, in *The Chemical Physics of Solid Surfaces*, edited by D. A. King and D. P. Woodruff (Elsevier, Amsterdam, 1993), Vol. 6, pp. 29–49.

²H. P. Bonzel and G. Pirug, in *The Chemical Physics of Solid Surfaces* (Ref. 1), p. 108.

³E. Bertel *et al.*, Phys. Rev. B **52**, 14 384 (1995); E. Bertel *et al.*, Ber. Bunsenges. Phys. Chem. **100**, 114 (1996).

⁴N. Memmel and E. Bertel, Phys. Rev. Lett. **75**, 485 (1995).

⁵K. Kern *et al.*, Surf. Sci. **175**, L669 (1986).

⁶R. Roos *et al.*, Chem. Phys. Lett. **232**, 537 (1995).

⁷G. Pirug and H. P. Bonzel, Surf. Sci. **194**, 159 (1988).

⁸E. L. Garfunkel and G. A. Somorjai, Surf. Sci. **115**, 441 (1982).

⁹C. M. Greenlief *et al.*, Surf. Sci. **186**, 563 (1987).

¹⁰R. G. Windham *et al.*, J. Phys. Chem. **92**, 2862 (1988).

¹¹K. Harrison *et al.*, Surf. Sci. **176**, 530 (1986).

¹²In principle, one could also determine the QMS signal from neutrals by means of a negative sample bias. However, field penetration could cause problems, because it would change the sensitivity towards neutrals.

¹³M. Kiskinova *et al.*, Surf. Sci. **133**, 321 (1983).

¹⁴P. Sandl, Doctoral thesis, University of Bayreuth, 1993.

¹⁵K. Christmann *et al.*, Surf. Sci. **152/153**, 356 (1985).

¹⁶E. Schweizer, Ph.D. thesis, Freie Universität Berlin, 1986.

¹⁷J. V. Barth *et al.*, Surf. Sci. Lett. **302**, L319 (1994).

¹⁸J. V. Barth *et al.*, Surf. Sci. **341**, 62 (1995).

¹⁹L. Q. Jiang *et al.*, Surf. Sci. **273**, 273 (1992).

²⁰K. Wandelt, in *Thin Metal Films and Gas Chemisorption*, edited by P. Wissmann (Elsevier, Amsterdam, 1987), p. 280–368.

²¹W. Friess, E. Steinacker, T. Brunner, and D. Menzel, Surf. Sci. Lett. **298**, L173 (1993), and references therein.

²²H. Over *et al.*, Surf. Rev. Lett. **2**, 409 (1995).

²³R. Fasel and J. Osterwalder, Surf. Rev. Lett. **2**, 359 (1995).

²⁴C. Stampfl *et al.*, Surf. Sci. **307-309**, 8 (1994); C. Stampfl and M. Scheffler, Surf. Rev. Lett. **2**, 317 (1995).

²⁵J. V. Barth *et al.*, Surf. Sci. Lett. **292**, L769 (1993).

²⁶R. J. Needs and M. Mansfield, J. Phys. Condens. Matter **1**, 7555 (1989).